



Utilization of the agricultural waste (*Cicer arietinum* Linn fruit shell biomass) as biosorbent for decolorization of Congo red

L. Sivarama Krishna^{a,b,*}, A. Sreenath Reddy^b, A. Muralikrishna^c, W.Y. Wan Zuhairi^a, Hasnah Osman^c, A. Varada Reddy^{b,*}

^aFaculty of Science and Technology, Department of Geology, School of Environmental Sciences and Natural Resources, Universiti Kebangsaan Malaysia, Bangi 43600, Selangor, Malaysia, Tel. +60 389215399; email: svurams@gmail.com (L. Sivarama Krishna), Tel. +60 389215390; email: yaacobzw@ukm.edu.my (W.Y. Wan Zuhairi)

^bAnalytical Division, Department of Chemistry, Sri Venkateswara University, Tirupati 517 502, AP, India, Tel. +91 9441408851; emails: sreesvuphd@gmail.com (A. Sreenath Reddy), ammireddy@yahoo.co.in (A. Varada Reddy)

^cSchool of Chemical Sciences, University of Sains Malaysia, Pulau Pinang 11800, Penang, Malaysia, Tel. +60 389215390; email: amreddymc@gmail.com (A. Muralikrishna), Tel. +60 46533558; email: osman.hasnah2012@yahoo.com (H. Osman)

Received 22 February 2014; Accepted 19 August 2014

ABSTRACT

Investigations have been carried out to study the use of Bengal gram fruit shell (SP) as a low-cost, eco-friendly biosorbent for the removal of Congo red (CR) from aqueous solution. Fourier transform infrared spectrometer and SEM were used to carry out characteristic studies on the material prepared. The effects of solution pH, biosorbent dosage, dye concentration, temperature, and contact time on the biosorption of CR onto the SP were investigated. The experimental results showed that maximum pH for efficient CR biosorption was about 8.0. Langmuir and Freundlich isotherm models were used for analyzing the equilibrium data. The maximum monolayer biosorption capacity was found as 22.22 mg g^{-1} at 35°C . Kinetic studies indicated that the pseudo-second-order model fitted the experimental data well. Thermodynamic parameters demonstrated that the biosorption process was spontaneous and endothermic. The results revealed that the SP could be used as a low-cost and eco-friendly alternative biosorbent for the CR removal from wastewater.

Keywords: Bengal gram fruit shell (SP); Agricultural by-product; Congo red; Thermodynamic parameters; Kinetics; Adsorption models; Wastewater treatment

1. Introduction

Color is the first contaminant to be recognized in wastewater. The presence of even a very small amount of dye in water is highly visible and undesirable [1]. Dyes are having a wide range of applications and are used in many industries for coloring purpose [2,3]. These industries produce large volume of wastewater,

containing several kinds of synthetic dyestuffs which cause serious ecological and environmental problems due to their potential toxicity [4].

Synthetic dyes are highly visible and biodegradable even if present in small amounts in water, because they have complex aromatic structures [5]. These colored dye effluents are considered to be highly toxic to the aquatic life and to reduce photosynthetic activity, due to the colorization of the water.

*Corresponding authors.

Therefore, it is necessary to treat them before discharging them into the water bodies [6,7].

Many treatment methods are available for dye removal, from dye-containing wastewaters. But, adsorption is considered to be an effective and economical method for wastewater treatment. Adsorption technique is quite popular, due to its simplicity and high efficiency in the removal of pollutants from the water and wastewater [8,9]. Activated carbons are effective adsorbents for dye and metal removal, due to their excellent adsorption capacity, as they have more surface area [10]. But the usage of these materials is restricted due to its high cost and the regeneration cost is also very high. Hence, removal of pollutants from the water and wastewater remains a challenge to the researchers. The main aim of this paper is to introduce a viable alternative to the commercial activated carbons.

Various non-conventional adsorbents have been attempted and used for the removal of dyes from the polluted wastewater [11,12]. A number of non-conventional adsorbents such as Indian jujuba seeds [13], tamarind fruit shell powder [14], Cattail root [15], raw pine and acid-treated pine cone powder [16], nanocrystalline MFe_2O_4 ($M = Mn, Fe, Co, Ni$) spinel ferrites [17], cashew nut shell [18], jute stick powder [19], wheat bran and rice bran [20], Orange peel [21], montmorillonite [22,23], bentonite [24,25], rice hull ash [26], azadirachta indica leaf powder [27], fly ash [28], activated red mud [29], rice husk [30], fungi [31,32], coir pith carbon [33], mesoporous activated carbons [34], aniline propyl silica xerogel [35], alternanthera bettzchiiana plant powder [36], chitosan [37], and mesoporous Fe_2O_3 [38] have been used for the removal of CR from aqueous solutions.

Congo red (CR) is a benzidine-based anionic diazo dye. This dye contains two azo groups. These azo groups are toxic to many organisms and are suspected to be carcinogen and mutagen [39–41]. CR is a human carcinogen and it is banned in many countries because of health concerns. But, it is still widely used in several countries. Synthetic dyes in general and CR in particular are difficult to biodegrade, due to their complex aromatic structures, which provide them physicochemical, thermal, and optical stability [42]. Therefore, there is an urgent requirement for development of innovative, but low-cost processes, by which dye molecules can be economically removed.

In the present paper, Bengal gram (*Cicer arietinum* Linn) fruit shell biomass (SP) has been used for the removal of CR and used as an effective low-cost eco-friendly new adsorbent in the wastewater treatment. This material is called as Seniga Pottu (SP) in telugu and therefore, it is abbreviated as SP. This material is

found to be very useful and cost effective for a better removal of CR.

2. Materials and methods

2.1. Adsorbate

CR is an anionic dye with a molecular formula of $C_{33}H_{22}N_6Na_2O_6S_2$ was purchased from Sigma-Aldrich. The structure of CR is shown in Fig. 1. The CR used in the present study has a molecular weight of 696.7 g mol^{-1} with its maximum absorbance at a wavelength of 497 nm. The IUPAC name of CR is [1-naphthalene sulfonic acid, 3,3'-(4,4'-biphenylenebis(azo)) bis(4-amino-) disodium salt]. CR contains $-NH_2$ and $-SO_3^-$ functional groups. In this study, double distilled water was used for the preparation of dye solutions and in the total experiment. Dilutions were made wherever required, with double distilled water.

2.2. SP (*Cicer arietinum* Linn fruit shell) biosorbent

The fruit shell/Pod coats of *Cicer arietinum* Linn were collected in the agricultural fields in a village, named Parumanchala, which is about 50 km away from Kurnool city, during the harvesting season, in the last summer season (2009). The unwanted materials like weeds, bristles, etc. were separated and only big pieces of fruit shell were extensively washed in running tap water for removing earthy matter, dirt, particulate matter, etc. It was followed by washing with double distilled water. The washed material was dried, under sun light, for 24 h. It was ground in pulverized mill. The fine ground powder was passing through $53 \mu\text{m}$ sieve and the material particle size, $<53 \mu\text{m}$ was prepared for the experimental studies. This material was stored in airtight pearl pet plastic containers. No other chemical or physical treatments were applied prior to adsorption experiments. In all the experiments, $<53 \mu\text{m}$ size SP was used. The biosorbent is shown in the Fig. 2.

2.3. Adsorption kinetics experimental methods and measurements

Adsorption experiments were carried out under batch mode at initial pH of dye. Initially, the effect of

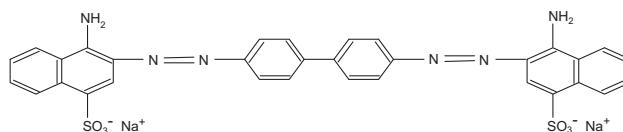


Fig. 1. Chemical structure of CR.



Fig. 2. (a) Plant of SP (*Cicer arietinum* Linn) and (b) Biomass of SP.

pH on biosorption capacity of adsorbate (CR) onto SP was carried out. For the pH effect, pH of each solution was adjusted, using required quantity of 1 N HCl (or) 1 N NaOH, before mixing the biosorbent. The effect of initial concentration and temperature of the adsorbate solution was studied at initial pH. In a set of 50 mL screw-type Erlenmeyer flask, containing biosorbate and solution, 25 mL of particular initial concentration was taken. Fixed dose (0.1 g/25 mL) of biosorbent was added to the adsorbate solutions. Each sample was agitated in an incubating shaker (Thermostatic Julabo water bath shaker) at a particular temperature. Samples at different time intervals were withdrawn and the supernatant of dye solution was separated by centrifuging (10,000 rpm) and the filtrate was analyzed for the residual CR concentration using UV–visible spectrophotometer (Chemito UV–vis Spectrophotometer) at the maximum wavelength of 497 nm of the dye.

The amount of biosorption at time t and at equilibrium time and the percentage of dye removal were calculated following Eqs. (1) and (2).

$$q_t = [(C_0 - C_t)V]/W \quad (1)$$

where C_0 and C_t (mg L^{-1}) are the liquid phase concentrations of dye at initial and at any time t , respectively. V is the volume of the solution (L) and W is the mass of dry biosorbent used (g).

The dye removal percentage is to be calculated as follows:

$$\text{Removal percentage} = [(C_0 - C_e)/C_0] \times 100 \quad (2)$$

where C_e is the equilibrium concentration in solution (mg L^{-1}).

2.3.1. Biosorbent (SP) characterization

Scanning electron microscopy (JEOL 6510 LV-Japan) characterization was carried out to observe the surface texture. To resolve the functional groups and their wave numbers, spectra analysis was done for SP before and after treatment (SP-CR) using Fourier transform infrared spectrometer (FTIR) (Model JASCO FTIR-5300 Series) in the range of $400\text{--}4,000\text{ cm}^{-1}$. In these analyses, finely ground biosorbent with pressed pellets was prepared by grinding the powder specimens, with IR grade KBr in an agate mortar.

2.3.2. Error analysis

Due to the inherent bias, resulting from linearization of the isotherm model, the non-linear regression Chi-square (χ^2) test was employed as a criterion for the fitting quality. This statistical analysis is based on the sum of the squares of the differences between the experimental and model calculated data, of which each squared difference was divided, by the corresponding data obtained by calculating from models [29]. The χ^2 can be represented by Eq. (3).

$$\chi^2 = \sum (q_e - q_m)^2 / q_m \quad (3)$$

where q_e is the equilibrium capacity of the adsorbent, obtained from the experiment (mg g^{-1}) and q_m is the calculated equilibrium capacity according to the dynamic model (mg g^{-1}). A low value of χ^2 indicates that experimental data fit better to the value from the model. In order to confirm the best-fit isotherms and kinetic models, for the adsorption system, there is a need to analyze the data-set using the χ^2 .

2.4. Theory

2.4.1. Adsorption isotherm

To simulate the adsorption isotherm, two commonly used models, the Langmuir and Freundlich isotherms [13] were selected to understand the CR–SP interaction.

2.4.1.1. Langmuir isotherm.

$$(C_e/q_e) = (1/Q_{max}K_L) + (C_e/Q_{max}) \quad (4)$$

where q_m is the maximum amount of biosorption (mg g^{-1}), K_L is the Langmuir constant related to the energy of adsorption (L mg^{-1}).

The Langmuir constants K_L and q_m can be determined from the linear plot of C_e vs. C_e/q_e .

2.4.1.2. Freundlich isotherm. Freundlich isotherm model is also applied to describe the adsorption of dye. Linearized in logarithmic form of Freundlich isotherm model equation is represented by:

$$\log q_e = \log K_F + (1/n) \log C_0 \quad (5)$$

where q_e is the amount of dye adsorbed per unit of adsorbent at equilibrium (mg g^{-1}), C_e is the concentration of dye solution at equilibrium (mg L^{-1}), K_F is the Freundlich constant, $1/n$ is the heterogeneity factor.

The adsorption isotherm constants, being indicative of the extent of the adsorption and the degree of non-linearity between solution concentration and adsorption, respectively. K_F and $1/n$ values can be calculated from intercept and slope of the linear plot between $\log C_e$ and $\log q_e$.

R_L , a dimensionless constant, is used to determine whether biosorption is favorable, or not, which is calculated by:

$$R_L = 1/(1 + K_L C_0) \quad (6)$$

2.4.2. Adsorption kinetics

Adsorption kinetic models were applied to interpret the experimental data, to determine the controlling mechanism of dye biosorption from aqueous medium.

2.4.2.1. Pseudo-first-order model. Pseudo-first-order equation or Lagergren's kinetics equation [17] is widely used for the adsorption of biosorbate from an aqueous solution. This kinetic is based on the assumption that

the rate of change of solute uptake with time is directly proportional to the difference in saturation concentration and the amount of solid uptake with time.

$$\log(q_e - q_t) = \log q_e - (K_1/2.303)t \quad (7)$$

where k_1 is the rate constant of pseudo-first-order biosorption (min^{-1}), q_e is the amount of dye adsorbed on biosorbent at equilibrium, q_t is the amount of dye biosorbed per unit of biosorbent (mg g^{-1}) at time, t is the contact time (min).

The biosorption rate constant (k_1) was calculated from the slope of plot of $\log (q_e - q_t)$ against t .

2.4.2.2. Pseudo-second-order model. Senthil Kumar et al. [18] presented the pseudo-second-order kinetics as:

$$t/q_t = (1/k_2 q_e^2) + (1/q_e)t \quad (8)$$

where k_2 is the rate constant of pseudo-second-order biosorption ($\text{g mg}^{-1} \text{min}^{-1}$). The q_e and k_2 can be obtained by linear plot of t/q_t vs. t .

2.4.2.3. Intraparticle diffusion model. Intraparticle diffusion model is commonly used for identifying the adsorption mechanism for design purposes. The effect of intraparticle diffusion resistance on biosorption can be determined by the following relationship [13]:

$$q_t = k_{pi} t^{0.5} + C_i \quad (9)$$

where k_{pi} is the rate parameter of stage ($\text{mg g}^{-1} \text{min}^{-0.5}$), C_i is the thickness of the boundary layer.

To follow the intraparticle diffusion model, a plot of q_t against $t^{0.5}$ should give a straight line where the slope is k_{pi} and intercept C_i . Values of C_i give information, regarding the thickness of boundary layer, i.e. the larger intercept the greater is the boundary layer effect.

2.4.2.4. Thermodynamic study. Thermodynamic parameters such as Gibb's free energy (ΔG°), enthalpy changes (ΔH°), and change in entropy (ΔS°) for the adsorption of CR on SP have been determined using the following equations:

$$\Delta G^\circ = -RT \ln K_c \quad (10)$$

where

$$K_c = C_s/C_e \quad (11)$$

$$\ln K_c = (\Delta S^\circ/R) - (\Delta H^\circ/RT) \quad (12)$$

where C_s is the equilibrium concentration of CR on biosorbent (mg L^{-1}), C_e is the equilibrium concentration of CR in solution (mg L^{-1}), K_c is the equilibrium constant, R is the ideal gas constant ($8.314 \text{ J mol}^{-1} \text{ K}^{-1}$), and T is the biosorption temperature in Kelvin.

2.5. Determination of point zero charge (pH_{pzc})

The point zero charge was used to determine the point where the density of electrical charge is zero. We have followed the procedure, mentioned in our previous paper [13] for the determination of point zero charge of SP. The solid addition method used to determine the point zero charge of biosorbent (SP) is briefly discussed.

The solid addition method [43] was used to determine the point zero charge of the biosorbent. An amount of 0.1 g of SP was added to each conical flasks containing 25 mL of the KNO_3 (0.1 N) solution. The initial pH was adjusted in the range of 2–12 using KOH (0.1 N) and HNO_3 (0.1 N) solutions. After 24 h of shaking, all conical flasks were withdrawn from the shaker and allowed to equilibrate for 0.5 h. Afterward, the final pH of the solutions was recorded. The intersection point of the curve ΔpH ($\text{pH}_f - \text{pH}_i$) vs. pH_i is considered as the amount of point zero charge.

2.6. Effect of biosorbent mass (SP)

The effect of biosorbent (SP) mass quantity was studied, by varying the quantity of biosorbent in the range of 0.05–0.5 g, whereas the parameters such as initial dye concentration, contact time, pH of the solution, stirring rate, and temperature were all kept constant during the adsorption process. The effect of biosorbent mass was studied using a series of conical flasks each containing 25 mL of dye solutions with the initial concentration of 50 mg L^{-1} . The solution was shaken in a shaker, for 3 h, at room temperature. The residual concentration was measured to determine the optimum value of the biosorbent. Dye removal efficiency and percentage were calculated using the above Eqs. (1) and (2).

3. Results and discussion

3.1. Surface characterization of biosorbent (SP)

Scanning electron micrograph (SEM) of SP before and after biosorption is shown in Figs. 3 and 4, respectively. The availability of pores and internal surface is clearly displayed in the SEM picture of the SP, before

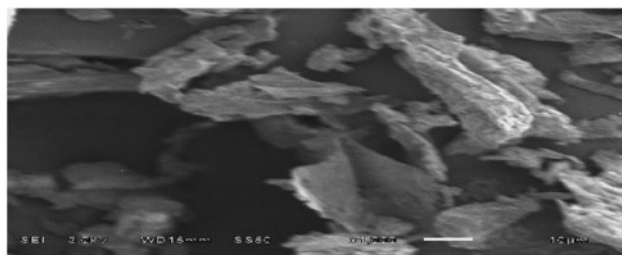


Fig. 3. Scanning electron microscopic photograph of SP.

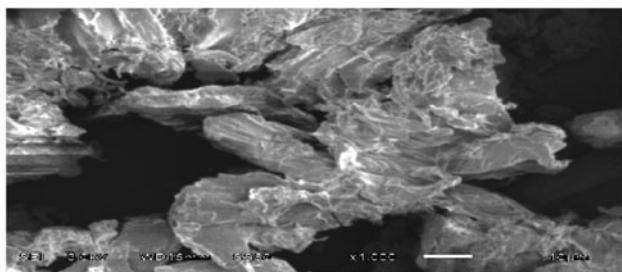


Fig. 4. Scanning electron microscopic photograph of CR-loaded SP.

biosorption and the coverage of the surface and the pores by the biosorbed CR is shown in Fig. 4. Basically, the porous structure that appears in Fig. 3 gets distorted in Fig. 4, because of the biosorption that occurs.

The biosorption of CR on SP was also affected by other interactions between functional groups of CR and SP, in addition to electrostatic interactions. FTIR analyses were conducted in order to identify possible locations for these interactions. Fig. 5 shows the FTIR spectra of SP and SP after adsorption of CR. FTIR spectra of SP shows the broad band centered $3,435.53 \text{ cm}^{-1}$ (stretching vibrations of the $-\text{OH}$ and $-\text{NH}$ groups), the band at $2,920.49 \text{ cm}^{-1}$ ($-\text{CH}_2$ asymmetric and symmetric stretching), the peak at $1,736.09 \text{ cm}^{-1}$ (associated with $\text{C}=\text{O}$ carbonyl), the peaks at $1,616.49$ and $1,421 \text{ cm}^{-1}$ (associated with the aromatic ring of

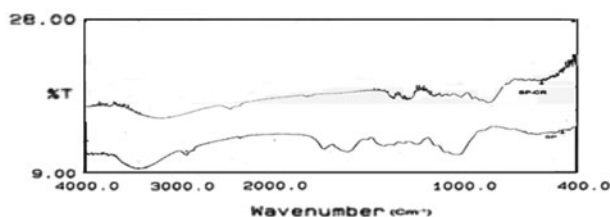


Fig. 5. FTIR spectra of (a) SP alone and (b) CR-loaded SP.

lignin), and the large peak at $1,033.94\text{ cm}^{-1}$ (associated with the C–O bond stretching of cellulose).

The main difference observed between the FTIR spectra of SP and the FTIR spectra of the SP loaded CR, after normalization, is a reduction, in the intensities for bands in the region between $3,435.53$ and $1,736.09\text{ cm}^{-1}$. The broad band $3,435.53\text{ cm}^{-1}$ is more reduced after biosorption, because the SP carboxyl and OH groups are associated with interactions of CR. It is observed that at $1,321.36$ and $1,249.99\text{ cm}^{-1}$ peaks are reduced after biosorption of CR and it may be due to the interactions between the carboxyl and OH groups of SP and the sulfonic acid groups of CR [41]. Fig. 6 shows the point zero charge that is around 5. pH_{pzc} was determined to understand the mechanism of biosorption process. Adsorption of cations is favored at above pH_{pzc} , whereas adsorption of anions is favored at below pH_{pzc} . pH_{pzc} of SP was determined by solid addition method [13], and it was found to be 5 (Fig. 6). This indicates that below this value, SP acquires positive charge due to protonation of functional groups, which result in electrostatic attraction between dye anions, whereas above this pH value a negative charge exists on the surface of SP. Hence, the biosorption of CR dye should be favorable at below pH_{pzc} because of the anionic nature of CR dye.

3.2. Effect of SP dose

The effects of biosorbent mass quantity on the removal of the CR shown in Fig. 7. The percentage of

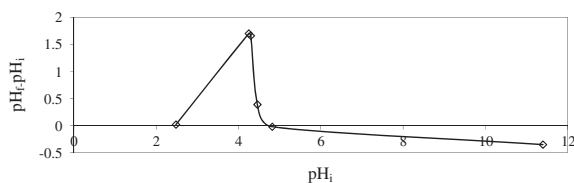


Fig. 6. Point zero charge (pH_{PZC}) of SP.

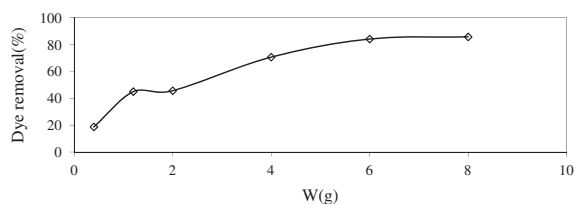


Fig. 7. Effect of biosorbent dose on the biosorption of CR on to SP.

Conditions: Agitation time = 3 h; $C_0 = 50\text{ mg L}^{-1}$; $V = 0.025\text{ L}$; temp. = $30 \pm 1^\circ\text{C}$; speed of agitation = 180 rpm; pH = 6.95; size of SP = $<53\text{ }\mu\text{m}$.

the CR adsorbed increased by increasing the mass of biosorbent from 18 to 85% for CR. As seen in Fig. 7, the biosorption efficiency increased, by increasing the biosorbent mass in the range of $0.4\text{--}8\text{ g L}^{-1}$ and reached the equilibrium state at a dosage of 4 g L^{-1} of biosorbent. An increase in biosorption may be concluded due to an increase in the biosorbent surface and therefore, more active functional groups resulting in the availability of more biosorption sites. The biosorption capacity decreased by increasing the amount of biosorbent due to the existence of the unsaturated biosorption sites, during the biosorption process. A biosorbent mass of 4 g L^{-1} was selected for further studies, as the optimal dosage.

3.3. Effect of pH

Effect of pH on the removal percentage rate of CR by the SP is shown in Fig. 8. The pH value of the dye solution plays an important role in the whole biosorption process and particularly on the biosorption capacity. Fig. 8 indicates that the percentage removal of dye was maximum in the pH range of 5–6 and decreased with further increase in pH value. This result is in agreement with the previously reported publications [13,28]. The SP material having the pH_{pzc} 5. The biosorption increased until it reached pH 5 and then was gradually decreased after pH 5.

At a pH of 6 and above, a decrease in biosorption takes place, due to the repulsion between anionic dye molecules and negatively charged biosorbent surface.

3.4. Effect of initial concentration and contact time

Fig. 9 shows the initial CR concentration which provides an important driving force to overcome all mass transfer resistance. Hence, a higher initial concentration of dye tends to enhance the biosorption process [25]. The biosorption of CR was rapid until 60 min and then the biosorption was gradual and finally attained saturation at equilibrium (180–300 min). The biosorption capacity of biosorbent increases when the

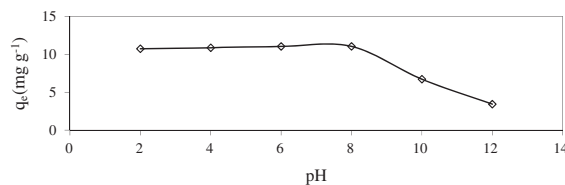


Fig. 8. Effect of pH on equilibrium uptake of CR. Conditions: Agitation time = 3 h; $C_0 = 50\text{ mg L}^{-1}$; $V = 0.025\text{ L}$; temp. = $30 \pm 1^\circ\text{C}$; speed of agitation = 180 rpm; size of SP = $<53\text{ }\mu\text{m}$.

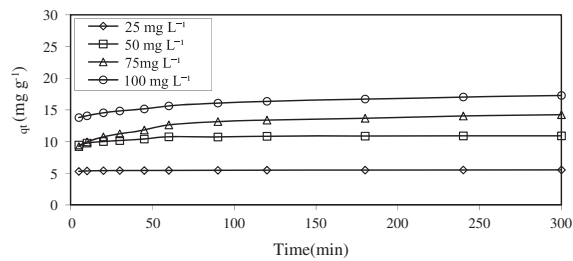


Fig. 9. Effect of initial concentration and contact time on CR adsorption.

Conditions: CR concentration: \diamond , 25 mg L⁻¹; δ , 50 mg L⁻¹; Δ , 75 mg L⁻¹; \circ , 100 mg L⁻¹; $V = 0.025$ L; temp. = 35 ± 1 °C; speed of agitation = 180 rpm; size of SP = <53 μm; dose = 0.1 g; pH = 6.95.

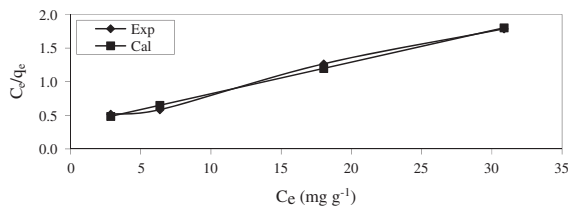


Fig. 10. Langmuir isotherm of CR on SP at 35 ± 1 °C.

initial CR concentration increases from 25 to 100 mg L⁻¹. Similar results have been reported previously in literature [13,44]. For the equilibrium biosorption capacity range of 25–100 mg L⁻¹, the initial CR concentrations were found to be 5.5345 to 17.2833 mg g⁻¹ for SP. The contact time is one of the most important parameters for practical application. According to Fig. 9, the CR was rapidly adsorbed in the first 60 min, and then the biosorption rate increased gradually from 60 to 300 min and finally reached the equilibrium in about 300 min [13]. The rapid biosorption at initial stage may be due to the fact that a large number of sites are available for biosorption of CR on SP. The slow rate of biosorption after first 60 min., probably occurred due to the fact that the active sites of the exterior surface reached saturation and the CR molecules entered into the pores of the SP.

Table 1

Isothermal parameter values for the biosorption of CR on SP at different concentrations and temperature of CR solution

Parameters	Langmuir constants				Freundlich constants			
	Q_{max} (mg g ⁻¹)	K_L (L mg ⁻¹)	R^2	χ^2	K_F	n	R^2	χ^2
Concn. of CR (mg L ⁻¹)	22.22	0.1111	0.9960	0.0376	3.3420	2.0534	0.9960	0.0279

Conditions: Size of SP = <53 μm; pH of CR soln. = 6.95; dose of Sp = 0.1 g; speed of agitation = 180 rpm.

3.5. Biosorption isotherm analysis

Biosorption isotherms are useful to understand the nature of the interaction between CR and SP used for the removal of CR from wastewater [45]. Fig. 10 shows the Langmuir isotherm for SP and the values of the Langmuir constants q_m , K_L , R^2 (correlation coefficient), and χ^2 are listed in Table 1. The isotherm is found to be linear, over the entire concentration range, with a good linear correlation coefficient ($R^2 = 0.996$) and small χ^2 , showing that the data correctly fit the Langmuir isotherm. This indicates that the surfaces of SP were covered by a monolayer of CR molecules. Similar behaviors are also found for the adsorption of CR on bentonite and red mud [25] and jute stick powder [19]. The biosorption capacity of SP was found to be 22.22 mg g⁻¹. The essential features of the Langmuir isotherm can be expressed in terms of a dimensionless constant called separation factor (R_L). The value of $R_L = 0.135$, the value of R_L in the range of 0–1 indicates the favorable uptake of the CR process. The Freundlich equation is basically an empirical equation and is employed to describe the heterogeneous systems. The magnitude of the component n gives an indication of the favorability and K_F (L g⁻¹) is the Freundlich constant, related to the bonding energy. The value of n between 1 and 10 indicates beneficial adsorption. The values of the Freundlich constants together with the correlation coefficient R_F^2 and χ^2 are presented in Table 1. Based on the correlation coefficient (R^2) value, the R_L^2 was equals to R_F^2 in biosorbent. The dimensionless constant R_L also falls within a favorable region limit between 0 and 1. It was indicated that the models fit well for the biosorption of CR on SP. Figs. 10 and 11 are Langmuir and the Freundlich plots for the biosorption of CR on SP, respectively.

3.6. Adsorption kinetics

The biosorption kinetics was evaluated using both the pseudo-first-order and the pseudo-second-order models, to determine the controlling mechanism of CR adsorption on to SP. Figs. 12 and 13 show the kinetics

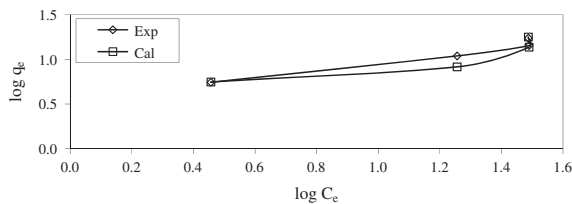


Fig. 11. Freundlich isotherm of CR on SP at $35 \pm 1^\circ\text{C}$.

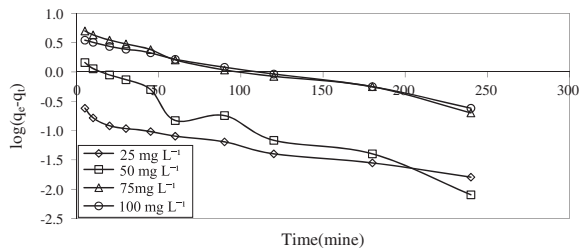


Fig. 12. Pseudo-first-order model for CR on SP for different initial concentrations.

Conditions: CR concentration: \diamond , 25 mg L^{-1} ; δ , 50 mg L^{-1} ; Δ , 75 mg L^{-1} ; \circ , 100 mg L^{-1} ; $V = 0.025\text{ L}$; temp. = $35 \pm 1^\circ\text{C}$; speed of agitation = 180 rpm ; size of SP = $<53\ \mu\text{m}$; dose = 0.1 g ; pH = 6.95 .

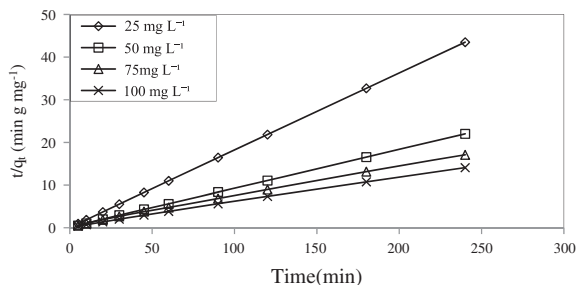


Fig. 13. Pseudo-second-order model for CR on SP for different initial concentrations.

Conditions: CR concentration: \diamond , 25 mg L^{-1} ; δ , 50 mg L^{-1} ; Δ , 75 mg L^{-1} ; \circ , 100 mg L^{-1} ; $V = 0.025\text{ L}$; temp. = $35 \pm 1^\circ\text{C}$; speed of agitation = 180 rpm ; size of SP = $<53\ \mu\text{m}$; dose = 0.1 g ; pH = 6.95 .

of CR biosorption, by using the pseudo-first-order and pseudo-second-order models. Kinetic parameters for pseudo-first-order and pseudo-second-order models values are shown in Table 2. The biosorption kinetics fits both the models. But, the calculated q_e ($q_{e\text{ cal}}$) values are slightly different from q_e ($q_{e\text{ exp}}$) for the pseudo-first-order when compared to that of pseudo-second-order model. R^2 value equal to 1 was obtained in case of pseudo-second-order model, at all CR concentrations. Therefore, the biosorption kinetics obeyed

pseudo-second-order model very well. It has been observed that most CR adsorption kinetics fits the pseudo-second-order model [15,19,46,47].

Intraparticle diffusion kinetic model was also used to examine CR biosorption by SP. As shown in Fig. 12, two/three stages for the CR biosorption were observed. The first sharper region is an instantaneous biosorption and is probably due to a strong electrostatic attraction between CR and the external surface of SP. The second stage is a gradual adsorption stage, which can be attributed to intraparticle diffusion of dye molecule, through the pores of biosorbent. The third region existed especially for high initial dye concentration, which was the final equilibrium stage, as the intraparticle diffusion started to slow down. Referring to Fig. 14, the plots were not linear over the whole time range. In other words, intraparticle diffusion was not the only rate-limiting mechanism in the biosorption process. The values are shown in Table 3. It is obvious from Table 3 that values of k_{pi} for first linear region increase slightly from 0.053 to 0.576 when the initial CR concentration is increased from 25 to 100 mg L^{-1} and a further increase to 100 mg L^{-1} has little effect. More or less similar trend is observed, for all the other linear regions. It was also observed that the value of the intercept increases when C_0 is increased from 25 to 100 mg L^{-1} . Similar results are also observed for the adsorption of CR on jujuba seeds [13].

3.7. Thermodynamic parameter

The effect of temperature on the biosorption of CR on SP was studied by performing the biosorption experiments at different temperatures ($35\text{--}65^\circ\text{C}$). The results revealed that the biosorption capacity increased with increase in temperature from 35 to 65°C , indicating the endothermic nature of dye biosorption.

Thermodynamic parameters are used for better understanding of the effect of temperature effect on dye biosorption on biosorbent. The thermodynamic parameters of biosorption process such as change in standard free energy (ΔG°), enthalpy (ΔH°), and entropy (ΔS°) were calculated using the 10, 11, and 12 equations and from Fig. 15. Table 4 shows the thermodynamic parameters for the biosorption of CR dye onto SP. The ΔH° value obtained is 16.14 kJ mol^{-1} . The positive sign indicates that the process is endothermic in nature. This behavior might be due to the increase of diffusion rate of CR across the external boundary layer and internal pores of SP. The biosorption of CR dye onto SP shows that the rate-limiting step in the process is physically controlled.

Table 2

Pseudo-first-order and pseudo-second-order rate constants at 35°C and different initial CR concentrations

C_0 (mg L ⁻¹)	$q_{e \text{ exp}}$ (mg g ⁻¹)	Pseudo-first-order model			Pseudo-second-order model		
		k_1 (min ⁻¹)	$q_{e \text{ cal}}$ (mg g ⁻¹)	R^2	K_2 (min ⁻¹)	$q_{e \text{ cal}}$ (mg g ⁻¹)	R^2
25	5.5345	0.0092	5.9073	1.0000	0.3485	5.5273	1.0000
50	10.9097	0.0207	10.9316	1.0000	0.0552	11.0041	1.0000
75	14.2436	0.0115	14.7084	0.9992	0.0107	14.3635	1.0000
100	17.2833	0.0092	18.4473	0.9994	0.0139	17.3011	1.0000

Conditions: Size of SP = <53 μm; pH of CR soln. = 6.95; dose of Sp = 0.1 g; speed of agitation = 180 rpm.

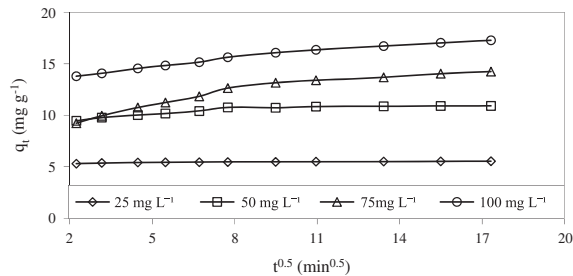


Fig. 14. Intraparticle diffusion kinetics for the biosorption of CR on SP.

Conditions: CR concentration: \diamond , 25 mg L⁻¹; δ , 50 mg L⁻¹; Δ , 75 mg L⁻¹; \circ , 100 mg L⁻¹; $V = 0.025$ L; temp. = 35 ± 1 °C; speed of agitation = 180 rpm; size of SP = <53 μm; dose = 0.1 g; pH = 6.95.

The positive values of ΔS° suggesting that during biosorption at the solid–liquid interface, the degree of freedom increased. Besides, the positive value indicates the randomness at solid–liquid interface reflecting the affinity of CR dye toward the SP. The negative value of ΔG° indicates that the biosorption process is spontaneous. ΔG° values obtained are lower than 20 kJ mol⁻¹; its indicating that the biosorption process follows physisorption mechanism. The values are shown in Table 4.

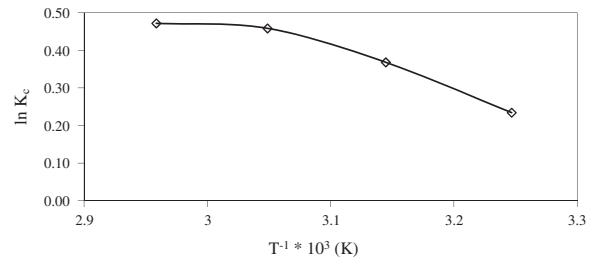
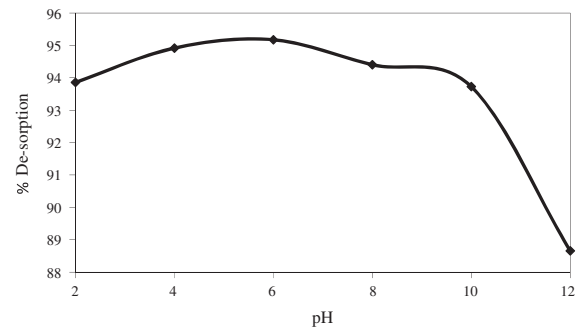
Fig. 15. Plot of $\ln K_c$ against T^{-1} for the removal of CR by SP.

Fig. 16. Desorption studies for the removal of CR.

Table 3

Intraparticle diffusion constants for different initial CR concentrations at 35°C

Linear portion ↓	Constants ↓	$C_0 = 25$ mg L ⁻¹	$C_0 = 50$ mg L ⁻¹	$C_0 = 75$ mg L ⁻¹	$C_0 = 100$ mg L ⁻¹
First	K_{P1} (mg g ⁻¹ min ^{-0.5})	0.0525	0.2177	0.5761	0.319
	C_1 (mg g ⁻¹)	5.1865	9.0179	8.0584	13.085
	R^2	0.9381	0.984	0.9904	0.9963
Second	K_{P2} (mg g ⁻¹ min ^{-0.5})	0.0121	0.0155	0.4583	0.1527
	C_2 (mg g ⁻¹)	5.3591	10.656	8.8876	14.662
	R^2	0.9936	0.9481	0.9304	0.9974
Third	K_{P3} (mg g ⁻¹ min ^{-0.5})	0.0062	–	0.1388	–
	C_3 (mg g ⁻¹)	5.4248	–	11.855	–
	R^2	0.9815	–	0.9953	–

Conditions: Size of SP = <53 μm; pH of CR soln. = 6.95; dose of Sp = 0.1 g; speed of agitation = 180 rpm.

Table 4
Thermodynamic parameters for the biosorption of CR on SP

Temp. (°C)	$K_c = C_s/C_e$	ΔG° (kJ mole ⁻¹)	ΔS° (kJ mole ⁻¹ K ⁻¹)	ΔH° (kJ mole ⁻¹)
35	0.8363	-4.9321	18.8519	16.1410
45	0.9703	-5.9078		
55	1.0605	-6.6602		
65	1.0739	-6.9502		

Conditions: Size of SP = <53 μm ; pH of CR soln. = 6.95; dose of SP = 0.1 g; speed of agitation = 180 rpm.

Table 5
Adsorption capacities of CR on various adsorbents

S. No.	Name of adsorbent	q_e (mg g ⁻¹)	Reference	Equilibrium time (h)	Temperature (°C)
1	Jujuba seeds	55.56	[13]	5	30
2	Jute stick powder	35.70	[19]	24	30
3	Sunflower stalks	31.5–37	[48]	3	21
4	Cattail root	38.79	[15]	24	20
5	Wheat bran	22.73	[20]	8.33	25
6	Rice bran	14.63	[20]	8.33	25
7	Tamarind fruit shell	10.48	[14]	7	30
8	<i>A. bettzichiiana</i> plant powder	14.67	[36]	2.10	30
9	Raw pine cone	32.65	[16]	3	30
10	Orange peel	7.90	[21]	3	29
12	Bagasse fly ash	11.88	[28]	4	30
13	Cashew nut shell	5.18	[18]	2	30
14	Ball-milled sugarcane bagasse	38.20	[8]	24	30
15	SP (Bengal gram fruit shell)	22.22	Present study	5	35

3.8. Desorption studies

Desorption studies help to elucidate the nature of biosorption and recycling of the spent biosorbent and the CR. In the desorption studies, the loaded biosorbent that was used for the biosorption of dye solution was separated from solution by centrifugation. The biosorbent along with adsorbate was agitated with 25 mL of distilled water, at different pH values (2–12) for 3 h. The amount of desorbed dye was determined. It was found that the desorption percentage increased with increasing pH value up to pH 6. After pH 6, the desorption percentage decreased as shown in Fig. 16. The desorption tests have shown that the maximum dye released was 95.18% at pH 6 and then decreased up to pH 12.

4. Comparison of various adsorbents

A lot of research work has been done on removal of CR from wastewater by using so many low-cost materials in addition to SP. The adsorption capacity of other adsorbents along with SP is shown in Table 5 for comparison purpose. The new biomass of SP having good biosorption capacity of CR, that is comparable with

other works on adsorption of CR, from other adsorbents. Therefore, SP is considered to be an excellent biosorbent for the removal of CR from aqueous solution.

5. Conclusions

The present study shows that biosorbent prepared from low-cost material, Bengal gram husk, is considerably efficient for removal of CR from wastewater. The adsorption is highly dependent on contact time, biosorbent dose, and pH. The most ideal pH for biosorption of CR dyes on SP is 6 and below. The kinetics of CR biosorption on SP follows the pseudo-second-order model. The equilibrium data fit well in the Langmuir model of biosorption, showing monolayer coverage of dye molecules at the outer surface of SP. The value for the maximum biosorption capacity, Q_{max} , is comparable with the values for conventional adsorbents reported in earlier studies. The results would be useful for treatment of spent textile dyeing wastewater for the removal of CR dye. This biosorbent (SP) represents an abundant available natural material that can be utilized as an effective, low-cost, and alternative biomass for CR removal from an industrial wastewater.

Acknowledgments

The main author L. Sivarama Krishna would like to acknowledge Sri Venkateswara University, Tirupati. Special acknowledgment to Universiti Kebangsaan Malaysia for financial support to conduct a postdoctoral research.

References

- [1] M. Doğan, M.H. Karaoğlu, M. Alkan, Adsorption kinetics of maxilon yellow 4GL and maxilon red GRL dyes on kaolinite, *J. Hazard. Mater.* 165 (2009) 1142–1151.
- [2] T. Robinson, G. McMullan, R. Marchant, P. Nigam, Remediation of dyes in textile effluent: A critical review on current treatment technologies with a proposed alternative, *Bioresour. Technol.* 77 (2001) 247–255.
- [3] M.R. Malekbala, S. Hosseini, S. Kazemi Yazdi, S. Masoudi Soltani, M.R. Malekbala, The study of the potential capability of sugar beet pulp on the removal efficiency of two cationic dyes, *Chemic. Engg. Res. Des.* 90 (2012) 704–712.
- [4] Y. Safa, H.N. Bhatti, Adsorptive removal of direct textile dyes by low cost agricultural waste: Application of factorial design analysis, *Chem. Engg. J.* 167 (2011) 35–41.
- [5] G. CRINI, Non-conventional low-cost adsorbents for dye removal: A review, *Bioresour. Technol.* 97 (2006) 1061–1085.
- [6] M. Ghaedi, A. Ansari, M.H. Habibi, A.R. Asghari, Removal of malachite green from aqueous solution by zinc oxide nanoparticle loaded on activated carbon: Kinetics and isotherm study, *J. Indu. Eng. Chem.* 20 (2014) 17–28.
- [7] M.S. Chiou, P.Y. Ho, H.Y. Li, Adsorption of anionic dyes in acid solutions using chemically cross-linked chitosan beads, *Dyes Pig.* 60 (2004) 69–84.
- [8] Z. Zhang, L. Moghaddam, I.M. O'Hara, W.O.S. Doherty, Congo red adsorption by ball-milled sugarcane bagasse, *Chem. Engg. J.* 178 (2011) 122–128.
- [9] S. Chatterjee, A. Kumar, S. Basu, S. Dutta, Application of response surface methodology for methylene blue dye removal from aqueous solution using low cost adsorbent, *Chem. Engg. J.* 181–182 (2012) 289–299.
- [10] A. Afkhami, T. Madrakian, A. Amini, Mo(VI) and W (VI) removal from water samples by acid-treated high area carbon cloth, *Desalination.* 243 (2009) 258–264.
- [11] S. Chatterjee, A. Kumar, S. Basu, S. Dutta, Application of response surface methodology for methylene blue dye removal from aqueous solution using low cost adsorbent, *Chem. Eng. J.* 181–182 (2012) 289–299.
- [12] S.J. Allen, G. McKay, J.F. Porter, Adsorption isotherm models for basic dye adsorption by peat in single and binary component systems, *J. Colloid Interface Sci.* 280 (2004) 322–333.
- [13] M.C. Somasekhara Reddy, L. Sivaramakrishna, A. Varada Reddy, The use of an agricultural waste material, Jujuba seeds for the removal of anionic dye (Congo red) from aqueous medium, *J. Hazard. Mater.* 203–204 (2012) 118–127.
- [14] M.C. Somasekhara Reddy, Removal of direct dye from aqueous solution with a novel adsorbent made from Tamarind Fruit Shell, an agricultural solid waste, *J. Sci. Indu. Res.* 65 (2006) 443–446.
- [15] Z. Hu, H. Chen, F. Ji, S. Yuan, Removal of Congo red from aqueous solution by cattail root, *J. Hazard. Mater.* 173 (2010) 292–297.
- [16] S. Dawood, T.K. Sen, Removal of anionic dye Congo red from aqueous solution by raw pine and acid treated pine cone powder as adsorbent: Equilibrium, thermodynamic, kinetics, mechanism and process design, *Water Res.* 46 (2012) 1933–1946.
- [17] L. Wang, J. Li, Y. Wang, L. Zhao, Q. Jiang, Adsorption capability for Congo red on nanocrystalline MFe_2O_4 ($M = Mn, Fe, Co, Ni$) spinel ferrites, *Chem. Eng. J.* 181–182 (2012) 72–79.
- [18] P. Senthil Kumar, S. Ramalingam, C. Senthamarai, M. Niranjana, P. Vijayalakshmi, S. Sivanesan, Adsorption of dye from aqueous solution by cashew nut shell: Studies on equilibrium isotherm, kinetics and thermodynamics of interactions, *Desalination* 261 (2010) 52–60.
- [19] G.C. Panda, S.K. Das, A.K. Guha, Jute stick powder as a potential biomass for the removal of Congo red and rhodamine B from their aqueous solution, *J. Hazard. Mater.* 164 (2009) 374–379.
- [20] X. Wang, J. Chen, Biosorption of Congo red from aqueous solution using wheat bran and rice Bran: Batch studies, *Sep. Sci. Technol.* 44 (2009) 1452–1466.
- [21] C. Namasivayam, N. Muniasamy, K. Gayatri, M. Rani, K. Ranganathan, Removal of dyes from aqueous solutions by cellulosic waste orange peel, *Bioresour. Technol.* 57 (1996) 37–43.
- [22] Z. Yermiyahu, I. Lapides, S. Yariv, Visible absorption spectroscopy study of the adsorption of Congo red by montmorillonite, *Clay Miner.* 38 (2003) 483–500.
- [23] L. Wang, A. Wang, Adsorption characteristics of Congo red onto the chitosan/montmorillonite nanocomposite, *J. Hazard. Mater.* 147 (2007) 979–985.
- [24] L. Lian, L. Guo, C. Guo, Adsorption of Congo red from aqueous solutions onto Ca-bentonite, *J. Hazard. Mater.* 161 (2009) 126–131.
- [25] E. Bulut, M. Özacar, İ.A. Şengil, Equilibrium and kinetic data and process design for adsorption of Congo red onto bentonite, *J. Hazard. Mater.* 154 (2008) 613–622.
- [26] K.S. Chou, J.C. Tsai, C.T. Lo, The adsorption of Congo red and vacuum pump oil by rice hull ash, *Bioresour. Technol.* 78 (2001) 217–219.
- [27] K.G. Bhattacharyya, A. Sharma, Azadirachta indica leaf powder as an effective biosorbent for dyes: A case study with aqueous Congo red solutions, *J. Environ. Manag.* 71 (2004) 217–229.
- [28] I.D. Mall, V.C. Srivastava, N.K. Agarwal, I.M. Mishra, Removal of congo red from aqueous solution by bagasse fly ash and activated carbon: Kinetic study and equilibrium isotherm analyses, *Chemosphere* 61 (2005) 492–501.
- [29] A. Tor, Y. Cengeloglu, Removal of Congo red from aqueous solution by adsorption onto acid activated red mud, *J. Hazard. Mater.* 138 (2006) 409–415.
- [30] R. Han, D. Ding, Y. Xu, W. Zou, Y. Wang, Y. Li, L. Zou, Use of rice husk for adsorption of Congo red from aqueous solution in column mode, *Bioresour. Technol.* 99 (2008) 2938–2946.

- [31] Y. Fu, T. Viraraghavan, Removal of Congo red from an aqueous solution by fungus *Aspergillus niger*, *Adv. Environ. Res.* 7 (2002) 239–247.
- [32] A.R. Binupriya, M. Sathishkumar, K. Swaminathan, C.S. Kuz, S.E. Yun, Comparative studies on removal of Congo red by native and modified mycelial pellets of *Trametes versicolor* in various reactor modes, *Bioresour. Technol.* 99 (2008) 1080–1088.
- [33] C. Namasivayam, D. Kavitha, Removal of Congo red from water by adsorption onto activated carbon prepared from coir pith, an agricultural solid waste, *Dyes Pig.* 54 (2002) 47–58.
- [34] E.L. Grabowska, G. Gryglewicz, Adsorption characteristics of Congo red on coal based mesoporous activated carbon, *Dyes Pigm.* 74 (2007) 34–40.
- [35] F.A. Pavan, S.L.P. Dias, E.C. Lima, E.V. Benvenutti, Removal of Congo red from aqueous solution by anilinepropylsilica xerogel, *Dyes Pigm.* 76 (2008) 64–69.
- [36] A.K. Patil, V.S. Shrivastava, *Alternanthera bettzichiana* plant powder as low cost adsorbent for removal of Congo red from aqueous solution, *Int. J. Chem. Tech. Res.* 2 (2010) 842–850.
- [37] S. Chatterjee, S. Chatterjee, B.P. Chatterjee, A.K. Guha, Adsorptive removal of congo red, a carcinogenic textile dye by chitosan hydrobeads: Binding mechanism, equilibrium and kinetics, *Colloids Surf. A* 299 (2007) 146–152.
- [38] C. Yu, X. Dong, L. Guo, J. Li, F. Qin, L. Zhang, J. Shi, D. Yan, Template-free preparation of mesoporous Fe_2O_3 and its application as absorbents, *J. Phys. Chem. C* 112 (2008) 13378–13382.
- [39] A. Afkhami, T. Madrakian, A. Amini, Z. Karimi, Effect of the impregnation of carbon cloth with ethylenediaminetetraacetic acid on its adsorption capacity for the adsorption of several metal ions, *J. Hazard. Mater.* 150 (2008) 408–412.
- [40] L.-G. Wang, G.-B. Yan, Adsorptive removal of direct yellow 161 dye from aqueous solution using bamboo charcoals activated with different chemicals, *Desalination* 274 (2011) 81–90.
- [41] M.K. Purkait, A. Maiti, S. DasGupta, S. De, Removal of Congo red using activated carbon and its regeneration, *J. Hazard. Mater.* 145 (2007) 287–295.
- [42] R. Han, D. Ding, Y. Xu, W. Zou, Y. Wang, Y. Li, L. Zou, Use of rice husk for the adsorption of Congo red from aqueous solution in column mode, *Bioresour. Technol.* 99 (2008) 2938–2946.
- [43] B.H. Hameed, Evaluation of papaya seed as a novel non-conventional low-cost adsorbent for removal of methylene blue, *J. Hazard. Mater.* 162 (2010) 939–994.
- [44] Y. Yang, G. Wang, B. Wang, Z. Li, Jia, Q. Zhou, Y. Zhao, Biosorption of acid black 172 and Congo red from aqueous solution by nonviable *Penicillium YW 01*: Kinetic study, equilibrium isotherm and artificial neural network modeling, *Bioresour. Technol.* 102 (2011) 828–834.
- [45] C. Xia, Y. Jing, Y. Jia, D. Yue, D. Ma, X. Yin, Adsorption properties of Congo red from aqueous solution on modified hectorite: Kinetic and thermodynamic studies, *Desalination* 265 (2011) 81–87.
- [46] V. Vimonses, S.M. Lei, B. Jin, C.W.K. Chow, C. Saint, Kinetic study and equilibrium isotherm analysis of Congo red adsorption by clay materials, *Chem. Eng. J.* 148 (2009) 354–364.
- [47] C. Namasivayam, D.J.S.E. Arasi, Removal of Congo red from wastewater by adsorption onto waste red mud, *Chemosphere* 34 (1997) 401–417.
- [48] G. Sun, X. Xu, Sunflower stalks as a adsorbents for color removal from textile wastewater, *Ind. Eng. Chem. Res.* 36 (1997) 808–812.